

# Correspondence between $\delta^{13}\text{C}$ and $\delta^{15}\text{N}$ in soils suggests coordinated fractionation processes for soil C and N

Jacques A. Nel · Joseph M. Craine ·  
Michael D. Cramer

Received: 14 June 2017 / Accepted: 14 November 2017 / Published online: 2 December 2017  
© Springer International Publishing AG, part of Springer Nature 2017

## Abstract

**Background and aims** Although a number of different factors influence C and N isotopic fractionation of organic matter, the  $\delta^{13}\text{C}$  and  $\delta^{15}\text{N}$  values of soil organic matter both tend to increase with soil depth, following similar trajectories. This similarity has not been investigated at the global scale. As microbial decomposition increases organic matter  $\delta^{13}\text{C}$  and  $\delta^{15}\text{N}$  values, soil isotopic values are hypothesized to generally increase with depth across local and global scales.

**Methods** Soil  $\delta^{13}\text{C}$  and  $\delta^{15}\text{N}$  values for 16 soil depth-profile sites were used for local-scale investigation, and 5447 global single-depth sites were used for global-scale investigation of the correspondence between  $\delta^{13}\text{C}$  and  $\delta^{15}\text{N}$ . Correlative and boosted regression tree analyses were used to determine the main drivers of the variance in soil  $\delta^{15}\text{N}$  globally and also the environmental association of variability in the correlation with depth between  $\delta^{13}\text{C}$  and  $\delta^{15}\text{N}$  at a number of sites.

**Results** Strong positive correlations between  $\delta^{13}\text{C}$  and  $\delta^{15}\text{N}$  values through soil profiles were found at a number of sites and were found to be independent of vegetation type. Globally, soil  $\delta^{13}\text{C}$  and  $\delta^{15}\text{N}$  values were also found to be significantly positively correlated across a wide range of climates and biomes.

**Conclusion** The global correspondences between  $\delta^{13}\text{C}$  and  $\delta^{15}\text{N}$  values may suggest a mechanistic link between  $\delta^{13}\text{C}$  and  $\delta^{15}\text{N}$  through the process of SOM decomposition and microbial processing and highlight the importance of soil-related processes in determining isotopic signals in soils. The variability in these soil processes should be considered when interpreting soil isotopic values of  $\delta^{13}\text{C}$  and  $\delta^{15}\text{N}$  as indicators of ecosystem sources of soil C and N and inferring vegetation inputs.

**Keywords**  $\delta^{15}\text{N}$  ·  $\delta^{13}\text{C}$  · Decomposition · Microbial · Soil profiles · Soil organic matter

---

Responsible Editor: Hans Lambers

**Electronic supplementary material** The online version of this article (<https://doi.org/10.1007/s11104-017-3500-x>) contains supplementary material, which is available to authorized users.

---

J. A. Nel (✉) · M. D. Cramer  
Department of Biological Sciences, University of Cape Town,  
Private Bag X1, Rondebosch 7701, South Africa  
e-mail: jacques.a.nel@gmail.com

J. M. Craine  
Jonah Ventures, Manhattan, KS 66502, USA

## Introduction

Soil  $\delta^{15}\text{N}$  values tend to decrease with increasing mean annual precipitation (MAP) and decreasing mean annual temperature (MAT) across a broad range of climate and ecosystem types (Amundson et al. 2003). To some extent, this variation in soil  $\delta^{15}\text{N}$  values is associated with vegetation inputs, given that foliar  $\delta^{15}\text{N}$  values range over 35‰ across plants globally (Craine et al. 2009). Soil  $\delta^{15}\text{N}$  values, however, increase with decreasing soil organic C as global soil organic C

concentrations also decline with increasing MAT and decreasing MAP (Craine et al. 2015b). As a consequence, the dependence of soil  $\delta^{15}\text{N}$  on MAP and MAT has been ascribed to this association of soil C with environmental variables and the consequences of these for microbial transformation of both C and N. Furthermore, soils with greater clay concentrations often have higher soil  $\delta^{15}\text{N}$  values. The dependence of soil  $\delta^{15}\text{N}$  on soil C and clay is through fractionation associated with decomposition of soil organic matter that might at least partially be due to better water retention by clay, further linking it with environmental variables (SOM; Craine et al. 2015b).

Like soil  $\delta^{15}\text{N}$ , global patterns of soil  $\delta^{13}\text{C}$  values are correlated with MAP and MAT (Lu et al. 2004), but also with soil texture (Sollins et al. 2009). The largest influence on soil  $\delta^{13}\text{C}$  values, however, is the  $\delta^{13}\text{C}$  value of the input of C to the soil organic carbon (SOC) pool, which is either directly or indirectly derived from primary productivity (Kuzyakov and Domanski 2000). As a consequence, soil  $\delta^{13}\text{C}$  has been used as a proxy for historical vegetation shifts in the distribution of  $\text{C}_3$  and  $\text{C}_4$  vegetation (Swap et al. 2004; Gillson et al. 2004; Kuzyakov et al. 2006; Gillson 2015). Despite these clear geographic differences, changes in soil  $\delta^{13}\text{C}$  with depth do not necessarily reflect historic changes in the relative inputs of  $\text{C}_3$  and  $\text{C}_4$  vegetation. Turnover processes during soil development also contribute to changes in soil  $\delta^{13}\text{C}$  (Cerling 1984; Balesdent et al. 1993; Qiao et al. 2014) with more decomposed SOC having higher  $\delta^{13}\text{C}$  values (Boström et al. 2007). Thus both soil  $\delta^{15}\text{N}$  and  $\delta^{13}\text{C}$  values are, at least partially, determined by soil processes (i.e. decomposition and mineralization via microbial processing of OM), which may link the patterns of fractionation of these isotopes in the soil. If soil N and C isotope patterns are at least partially linked through common soil processes (i.e. decomposition and mineralization), then we may expect coordinated changes in  $\delta^{15}\text{N}$  and  $\delta^{13}\text{C}$  values with depth through a soil profile.

The  $\delta^{13}\text{C}$  values of SOM through soil profiles commonly increase by 1–3‰ as depth increases below 0.2 m relative to that of the surface litter layer (Chen et al. 2005; Boström et al. 2007). The enrichment of  $^{13}\text{C}$  with depth has been shown to occur in tropical, temperate and boreal systems (Hobbie and Ouimette 2009). Although atmospheric  $\delta^{13}\text{CO}_2$  has declined by 1.5‰ over the past 100 years, this has been shown to contribute only marginally to the enrichment of soil  $\delta^{13}\text{C}$  with

depth (Ehleringer et al. 2000; Esmeijer-Liu et al. 2012). At least four hypotheses have been proposed for C isotope fractionation through soil profiles. Firstly, kinetic discrimination against  $^{13}\text{C}$  during respiration may result from microorganisms preferentially respiring  $\text{CO}_2$  that is  $^{13}\text{C}$ -depleted relative to the substrate, resulting in  $^{13}\text{C}$  enrichment of the remaining SOC (Ågren et al. 1996). Although some studies show large  $^{13}\text{C}$  depletion of the  $\text{CO}_2$  formed (e.g. Fernandez et al. 2003), others show no or only minor isotopic fractionation (e.g. Ekblad and Högberg 2000). Secondly, microorganisms are  $^{13}\text{C}$ -enriched by 2 to 4‰ compared to plant material (Hobbie et al. 1999) and thus influence SOM, resulting in decreasing C:N ratios with soil depth (Wallander et al. 2003), and compound-specific shifts in soil organic matter to higher  $\delta^{13}\text{C}$  values in products of microbial origin (Huang et al. 1996; Ehleringer et al. 2000). Thirdly, variable mobility (e.g. fulvic acids; Heil et al. 2000) and sorption of isotopes of dissolved organic C on soil particulates (especially clay) may contribute to soil  $\delta^{13}\text{C}$  profiles (Craine et al. 2015b), although some authors have questioned the significance of these mechanism (Boström et al. 2007). Finally, although preferential utilization of  $^{13}\text{C}$ -depleted compounds has been suggested (Boström et al. 2007), the more recalcitrant C fractions of plant biomass (e.g. lignin, lipids and cellulose) that accumulate at depth (Rovira and Vallejo 2002) are  $^{13}\text{C}$ -depleted relative to the whole plant (Wilson and Grinstead 1977), and thus cannot contribute to increased  $^{13}\text{C}$ -enrichment with depth (Wynn et al. 2006). Apart from this, some, or all, of these processes may thus contribute to determining soil  $\delta^{13}\text{C}$  values to variable extents in different ecological contexts.

As with  $\delta^{13}\text{C}$ ,  $\delta^{15}\text{N}$  values usually increases with soil depth, although occasionally maximum  $\delta^{15}\text{N}$  is evident at an intermediate depth possibly as a result of increased volatilization in this soil zone (Hobbie and Ouimette 2009) followed by a subsequent decline at greater depths. The degree of enrichment that  $\delta^{15}\text{N}$  undergoes through a soil profile can have a much broader range than  $\delta^{13}\text{C}$ . In arid and semi-arid systems where soil pH is high, surface  $\delta^{15}\text{N}$  values can be elevated by as much as 7‰ relative to deeper soils (Pataki et al. 2008). There are six potentially important mechanisms that influence  $\delta^{15}\text{N}$  values within soil profiles. Firstly, depletion of  $^{15}\text{N}$  by mycorrhizal fungi and transfer of that  $^{15}\text{N}$ -depleted N to plants (Hobbie and Ouimette 2009) results in the accumulation of  $^{15}\text{N}$ -enriched N derived from mycorrhizal fungi (Högberg 1997; Hobbie and Ouimette

2009). Secondly, depletion of  $^{15}\text{N}$  through enzymatic hydrolysis (Silfer et al. 1992), ammonification, nitrification, or denitrification and the associated fractionation during gaseous loss of  $^{15}\text{N}$ -depleted N-containing gas or leaching loss of  $^{15}\text{N}$ -depleted  $\text{NO}_3^-$  and the preferential utilization of  $^{14}\text{N}$  by plants, drives soil  $\delta^{15}\text{N}$  values up (Handley and Raven 1992; Austin and Vitousek 1998). Thirdly, mixing of soil N among different soil layers through bioturbation (Gabet et al. 2003) and trophic fractionation (i.e. faunal processes; Ponsard and Arditi 2000) could alter soil  $\delta^{15}\text{N}$  profiles. Fourthly, soil texture (i.e. clay) may moderate  $^{14}\text{N}$  gaseous loss pathways and/or the differential retention of  $^{15}\text{N}$ -enriched SOM (Craine et al. 2015b). Fifthly, preferential microbial utilization of  $^{14}\text{N}$  compounds could contribute to accumulation of  $^{15}\text{N}$ -enriched compounds deeper in the soil (Boström et al. 2007). Finally, N deposition has been shown to decrease  $\delta^{15}\text{N}$  values of soils because deposited N is typically depleted in  $^{15}\text{N}$ , although this effect is relatively small (Liu et al. 2017; Esmeijer-Liu et al. 2012).

SOM decomposition is thus common to both  $\delta^{13}\text{C}$  and  $\delta^{15}\text{N}$  fractionation in soil. At the global scale, climate influences decomposition through both temperature and moisture (Gholz et al. 2000). The SOM composition and nutrient concentrations (especially N) also strongly affect decomposition (Parton et al. 2007). Although most SOM is derived from plants, only a small fraction of the yearly litter and root inputs are incorporated into the stable organic matter pool, most of it after repeated processing by soil microbes (Lerch et al. 2011). SOM transport through soils is generally downward through advection and soil development, and thus the effects of decomposition on soil  $\delta^{13}\text{C}$  and  $\delta^{15}\text{N}$  values are more noticeable deeper in the soil profile. With increasing depth, SOM is more highly processed by microbes (Trumbore 2009) with lower C:N ratios (Marin-Spiotta et al. 2014) and increasing  $\delta^{13}\text{C}$  and  $\delta^{15}\text{N}$  values (Heil et al. 2000; Billings and Richter 2006). This change in  $\delta^{13}\text{C}$  and  $\delta^{15}\text{N}$  is often modelled as “Rayleigh distillation”, which predicts soil  $\delta^{13}\text{C}$  and/or  $\delta^{15}\text{N}$  values based on the soil  $[\text{C}]/[\text{N}]$  in order to account for microbial isotopic enrichment of SOM during decomposition (Mariotti et al. 1981; Baisden et al. 2002; Wynn et al. 2005; Fischer et al. 2008). This enrichment results from the kinetic fractionation during microbial processing (Dijkstra et al. 2006) with subsequent stabilization of products by fine mineral particles in soils (Wynn et al. 2006). This Rayleigh

distillation model, however, only pertains to closed systems, potentially ignoring continuous inputs (Fry 2006) that do occur in soils.

Although a number of different factors influence the isotopic fractionation of C and N isotopes,  $\delta^{13}\text{C}$  and  $\delta^{15}\text{N}$  values both increase with soil depth and commonly follow similar trajectories. We hypothesized that changes in soil  $\delta^{13}\text{C}$  and  $\delta^{15}\text{N}$  values are coordinated, possibly through decomposition-related processes, and that the scale of decomposition related changes in  $\delta^{13}\text{C}$  may confound interpretation of soil  $\delta^{13}\text{C}$  as indicative of prior  $\text{C}_3$  or  $\text{C}_4$  vegetation. Although the initial isotope composition of the organic matter is indisputably important, subsequent soil fractionation may result in  $\delta^{13}\text{C}$  and  $\delta^{15}\text{N}$  following similar trajectories in space and time. We therefore predict that changes in  $\delta^{13}\text{C}$  and  $\delta^{15}\text{N}$  values correspond with each other both locally through soil depths at a site and globally due to the extent of decomposition and other soil processing. In order to test these predictions, we compiled data from soil depth profiles from sixteen widely distributed sites and also conducted an analysis of global  $\delta^{13}\text{C}$  and  $\delta^{15}\text{N}$  variations in surface soils in order to determine relationships between soil isotopes with climate and soil properties.

## Methods

### Data sources

Data for soil  $\delta^{13}\text{C}$  and  $\delta^{15}\text{N}$  values were acquired from literature and by contacting individual researchers known to have collected soil isotope data in the past. Soil depth-profile data included  $\delta^{13}\text{C}$  and  $\delta^{15}\text{N}$  for mineral soils at multiple depths at a single site. A second independent dataset included both mineral soil  $\delta^{13}\text{C}$  and  $\delta^{15}\text{N}$  values at a single depth at a number of geographic locations. For each site, climate data were taken from the original source and also, using the geographic coordinates, from the 50-year climatic means (1950–2000) obtained from [www.worldclim.org](http://www.worldclim.org) (accessed Sep 2014) at ca. 1 km<sup>2</sup> resolution. Variables included were mean annual temperature (MAT), mean annual precipitation (MAP) and 17 other derived climatic variables (Supp. Table 1).

Potential evaporation (PET) was obtained from Trabucco and Zomer (CGIAR Consortium for Spatial Information, 2009. Accessed: <http://www.csi.cgiar.org>)

in which PET was modelled using the method of Hargreaves et al. (1985) with data from Hijmans et al. (2015) and verified by comparison with separate data sources. From the climatic data, the monthly PET was subtracted from monthly precipitation to obtain an index of water availability (P–PET) and averaged to obtain the annual average. Normalized difference vegetation index (NDVI) data was obtained from eMODIS TERRA (US Geological Survey Earth Resources Observation and Science Center), which is corrected for molecular scattering, ozone absorption and aerosols. The NDVI data spanned between 19/12/2009 to 18/12/2012 and was at a spatial resolution of 250 m. The data was averaged to obtain monthly and annual average values using the “raster” (Hijmans et al. 2015) and “RCurl” (Lang and Lang 2016) packages in R.

The fraction of the vegetation with  $C_4$  photosynthesis was obtained from Berry et al. (2009) in which the percentage of vegetation within each one degree by one degree grid cell of the land surface which possesses the  $C_4$  photosynthetic pathway was determined using ‘ $C_4$  climate map’ from Collatz et al. (1998), ‘Continuous fields of vegetation characteristics’ from DeFries et al. (2000) as well as ‘Cropland fraction distribution’ from Ramankutty and Foley (1998). Where necessary, the component fields were re-sampled to bring them to a common one degree by one-degree spatial resolution.

The “SoilGrids1km” global soil data product (Hengl et al. 2014), which has mean soil information at 1 km resolution for six soil depths to 1.5 m deep (ISRIC – World Soil Information 2013), was averaged across the full depth by depth weighted-averaging. The environmental data included in the models is shown in Supp. Table 1.

#### Soil depth data

Data for 9 sites, which include 4 sites in Africa (Paulshoek, Pretoriuskop, Satara, Hluhluwe) and sites in Alaska, France, Sweden, New South Wales and the Amazon in Brazil were compiled from a number of publications (Table 1). These made up a total of 16 different sampling groups within distinct vegetation types and included data for 79 soil profiles at multiple depths. As most sites were represented by repeated sampling of different vegetation types, the average value of the N and C isotopes at each depth for each vegetation type, as well as the confidence intervals, were determined for each site. As the ranges of  $\delta^{13}C$  and  $\delta^{15}N$  values through soil profiles were different in magnitude,

the actual measured values were scaled using the “scale” function in R (z-transformation). This allowed both the N and C isotope patterns through the soil profiles to be plotted on the same set of axes for comparison using the ‘ggplot2’ package (Wickham 2009) in R. A Pearson correlation test was then performed on the scaled data. This correlation was then treated as a derived variable. As one of the locations, Hluhluwe, consisted of a number of different vegetation types, each vegetation type at the site was plotted separately rather than averaging across the site.

#### Global analysis of surface soil

In order to determine the main global correlates of soil  $\delta^{15}N$  values, the dataset from Craine et al. (2015b), which included soil and climatic data for sites around the globe, was re-analysed. Records that did not include a depth or mineral soil components were removed leaving a total of 5447 sites for the analysis. As the  $\delta^{13}C$  and  $\delta^{15}N$  values were from single depths only, the dataset was used to determine the global correlation of soil  $\delta^{13}C$  and other variables with  $\delta^{15}N$ .

#### Boosted regression tree analyses

Boosted regression tree models were used to determine how differences in soil and environmental conditions influence the correlation between  $\delta^{13}C$  and  $\delta^{15}N$  values for soil depth-profiles, as well as the main drivers of  $\delta^{15}N$  at the global scale. Boosted regression tree analysis is a form of non-linear modelling that uses machine learning (Elith et al. 2008). The modelling entails decision trees splitting the data into two homogenous groups, a process repeated many times (boosting) so as to improve the prediction of the response variable. Models are parameterized by adjusting their learning rates, tree complexity and bag fraction (Elith et al. 2008). We used a cross-validation procedure to identify the optimal number of trees and tree size for the model, and to guard against over-fitting (Hastie et al. 2001). Initially, the data set was randomly divided into 10 mutually exclusive subsets of equal size, 9 of which were used as a training set to create the boosted tree while the remainder was used as a test set to determine the predictive accuracy of the model. The data in the training sets were fitted using trees of different sizes (range = 2 to 10) by incrementally adding trees in sets of 50. For each combination of tree size and number of trees,

**Table 1** List of sites used in determining the correlation between soil  $\delta^{13}\text{C}$  and  $\delta^{15}\text{N}$  values through soil profiles. Variables included are mean annual temperature (MAT), mean annual precipitation (MAP),  $\delta^{15}\text{N}$ ,  $\delta^{13}\text{C}$ , the dominant vegetation at the site, the

Pearson correlation coefficients between  $\delta^{13}\text{C}$  and  $\delta^{15}\text{N}$  through soil profiles with significance values (bold where significant,  $p < 0.05$ ). Values for  $\delta^{13}\text{C}$  and  $\delta^{15}\text{N}$  are include the 5 percentiles, (means) and 95 percentiles of the soil profile data

Site	MAT (°C)	MAP (mm)	$\delta^{15}\text{N}$ (‰)	$\delta^{13}\text{C}$ (‰)	$\text{C}_3/\text{C}_4$ dominant	Pearson correlation	$p$ -value	Reference
Alaska	-4.1	405	-1.9 (0.1) 1.1	-27.0 (-24.4) -25.3	C3	0.98	<b>0.003</b>	Pries et al. 2012
Amazon	24.1	2134	8.2 (9.8) 11.1	-27.6 (-26.7) -25.9	C3	0.95	<b>0.000</b>	Ometto et al. 2006
Kruger - Satara OC	22.3	565	3.2 (6.1) 7.4	-13.7 (-12.3) -11.6	C4	0.94	<b>0.000</b>	February and Higgins 2010
Kruger - Satara UC	22.3	565	4.1 (6.0) 7.0	-15.0 (-13.0) -12.0	C4	0.92	<b>0.000</b>	February and Higgins 2010
Kruger - Pretoriuskop UC	21.0	734	2.0 (5.3) 6.9	-20.8 (-16.6) -14.5	C4	0.87	<b>0.000</b>	February and Higgins 2010
France - Natural	9.0	1280	1.7 (3.5) 4.7	-28.4 (-27.8) -27.2	C3	0.85	<b>0.071</b>	Zeller et al. 2007
Hluhluwe - Thicket	21.2	892	5.3 (6.5) 7.6	-18.0 (-16.4) -15.0	C4	0.72	<b>0.000</b>	Grey 2011
Sweden - Plantation	5.8	617	2.5 (5.8) 7.5	-27.8 (-27.4) -26.8	C3	0.68	0.136	Boström et al. 2007
Hluhluwe - Forest	21.2	892	6.8 (7.3) 7.9	-20.0 (-17.4) -15.5	C4	0.61	<b>0.000</b>	Grey 2011
Hluhluwe - Savanna	21.2	892	5.6 (6.5) 7.2	-15.0 (-13.8) -12.3	C4	0.58	<b>0.000</b>	Grey 2011
Kruger - Pretoriuskop OC	21.0	734	2.2 (5.1) 6.4	-17.6 (-14.8) -13.3	C4	0.50	<b>0.000</b>	February and Higgins 2010
Hluhluwe - Grassland	21.2	892	7.4 (8.1) 9.0	-15.5 (-13.9) -12.7	C4	0.49	<b>0.001</b>	Grey 2011
New South Wales - Grove	17.6	259	8.9 (10.0) 10.6	-22.1 (-18.8) -13.4	C4	0.46	0.297	Macdonald et al. 2015
France - Plantation	9.0	1280	1.0 (3.2) 5.2	-27.2 (-26.9) -26.7	C3	0.29	0.641	Zeller et al. 2007
New South Wales - Inter grove	17.6	259	8.5 (9.1) 9.5	-22.8 (-18.3) -13.2	C4	0.25	0.586	Macdonald et al. 2015
Karoo - Paulshoek	18.9	118	8.6 (9.2) 9.6	-21.2 (-21.0) -20.7	C3	-0.40	<b>0.007</b>	Edmund February unpublished

the predictive accuracy of the model was determined by comparing values in the test set with those predicted by the model. This procedure was repeated 10 times so that all groups were used as cross-validation groups, and the mean predictive error calculated across all subsets for each level of complexity. The combination of tree size and tree number that produced the lowest predictive error was chosen for all subsequent analyses. Performance was evaluated by expressing the predictive deviance of 10-fold cross validation as a percentage of the null deviance.

Two different models were used, either to explain the correlation of  $\delta^{13}\text{C}$  and  $\delta^{15}\text{N}$  values at the local scale across soil depths (BRTlocal), or to explain the value of  $\delta^{15}\text{N}$  at the global scale for a single soil depth (BRTglobal). The climatic and soil variables listed in Supp. Table 1 were used as the predictor variables. The ‘select07’ function (Dormann et al. 2013) in R, was used to identify collinear predictors. In cases where the predictor variables were found to be strongly collinear with each other, the variable

with either the strongest correlation with the response variable, or the most biologically relevant, was retained. Following an initial run (learning rate = 0.01, tree complexity = 5, bagging fraction = 0.5), a simplification procedure was implemented (Elith et al. 2008) to eliminate variables with low influence (such as NDVI and PET). Both models were run ten times using the libraries ‘gbm’ (Ridgeway et al. 2013) and ‘dismo’ (Hijmans and van Etten 2014) packages in R. Model outputs were used to ascertain the relative influence and relationship of each predictor with the correlation between  $\delta^{13}\text{C}$  and  $\delta^{15}\text{N}$  at the local scale or  $\delta^{15}\text{N}$  at the global scale.

To account for  $\text{C}_3$  and  $\text{C}_4$  vegetation input into the SOM pool, global soil  $\delta^{13}\text{C}$  values were analyzed for bimodality using libraries ‘diptest’ (Maechler 2015) in R and cutoffs were calculated using the ‘mixtools’ (Benaglia et al. 2009).  $\delta^{13}\text{C}$  for  $\text{C}_3$  and  $\text{C}_4$  were then treated as separate sets of data on which BRT modeling for global  $\delta^{15}\text{N}$  values were independently reanalyzed.

## Results

### Isotopic variation with soil depth

For 11 out of 16 sampling groups analyzed, the variation in average soil  $\delta^{13}\text{C}$  and  $\delta^{15}\text{N}$  values with depth were significantly positively correlated with each other (Fig. 1, Table 1). For many of these sites, both  $\delta^{13}\text{C}$  and  $\delta^{15}\text{N}$  values increased with depth, with the majority of the increase occurring in the upper 10–20 cm of the profile. The range of variability for both isotopes was ca. 2–8‰ through the soil profiles and this range was independent of the average  $\delta^{13}\text{C}$  and  $\delta^{15}\text{N}$  signature

for the sites (Table 1). Within the relatively small geographic area of the Hluhluwe Nature reserve, the significant positive correlations between  $\delta^{13}\text{C}$  and  $\delta^{15}\text{N}$  values were independent of vegetation types comprising forest, grassland, savanna and thicket sites. Across all of these distinct vegetation types,  $\delta^{13}\text{C}$  and  $\delta^{15}\text{N}$  values increased similarly with depth (Fig. 2, Table 1). For these sites the range of variability for both isotopes was also ca. 2–8‰ with the majority of the increase in  $\delta^{13}\text{C}$  and  $\delta^{15}\text{N}$  values occurring within the upper ca. 20 cm of the soil. Although most sites had significant positive correlations between  $\delta^{13}\text{C}$  and  $\delta^{15}\text{N}$ , for 5 of the 16 sampling groups, changes in average soil  $\delta^{13}\text{C}$  and

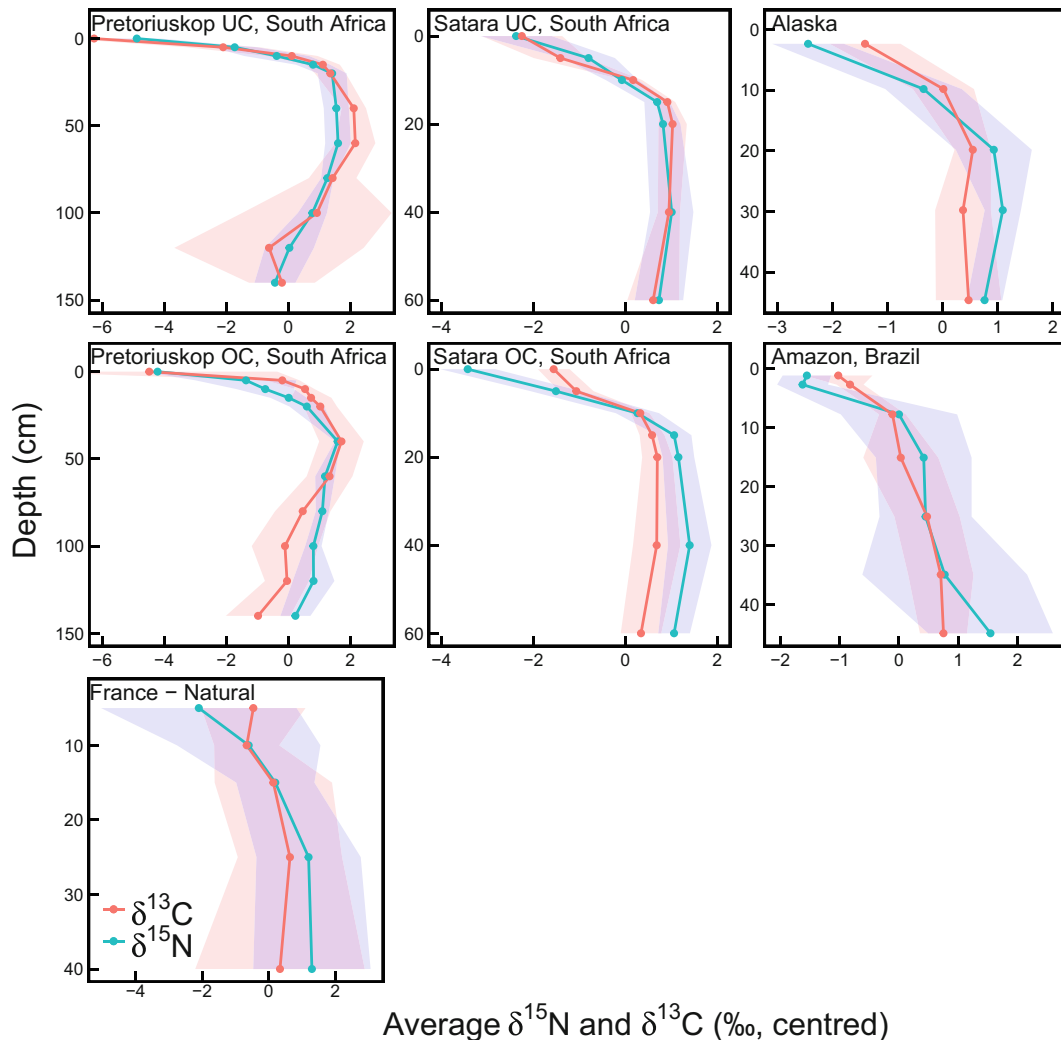
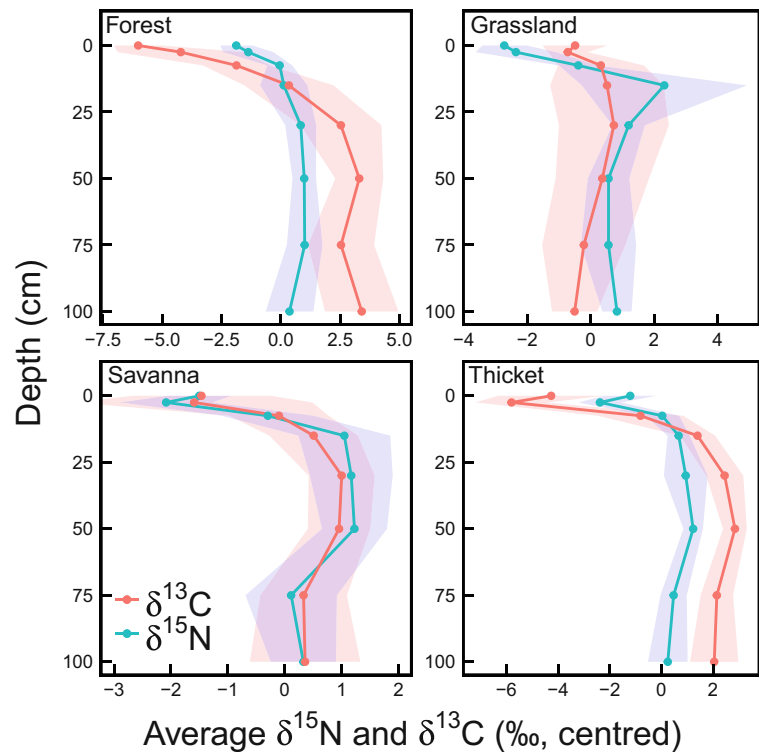


**Fig. 1** Variation with soil depth of  $\delta^{13}\text{C}$  and  $\delta^{15}\text{N}$  values for sites in which  $\delta^{13}\text{C}$  and  $\delta^{15}\text{N}$  are significantly correlated with each other (Table 1). The data was averaged for each depth and the confidence interval is represented by the coloured bands. The  $\delta^{13}\text{C}$  and  $\delta^{15}\text{N}$

data were independently centred on 0 so as to allow comparison of the variation of these within a site and thus the range of the data corresponds to that of the original data. Sites designated OC and UC are from open-canopy and under-canopy, respectively

**Fig. 2** Variation with soil depth of  $\delta^{13}\text{C}$  and  $\delta^{15}\text{N}$  values for sites in which the dominant vegetation types differ. The data was averaged for each depth and the confidence interval represented by the coloured bands. The  $\delta^{13}\text{C}$  and  $\delta^{15}\text{N}$  data were independently centred on 0 so as to allow comparison of the variation of these within a site and thus the range of the data corresponds to the original data



$\delta^{15}\text{N}$  values through the soil profiles were either not significantly associated or negatively correlated with each other (Fig. 3, Table 1). For these sites  $\delta^{13}\text{C}$  and  $\delta^{15}\text{N}$  values also increased with depth, with the exception of the Paulshoek site in which  $\delta^{15}\text{N}$  initially increased before subsequently decreasing below ca. 10 cm. These sites also had a wider range of  $\delta^{13}\text{C}$  and  $\delta^{15}\text{N}$  values than those for which there were significant correlations between  $\delta^{13}\text{C}$  and  $\delta^{15}\text{N}$  (Figs. 1, and 2).

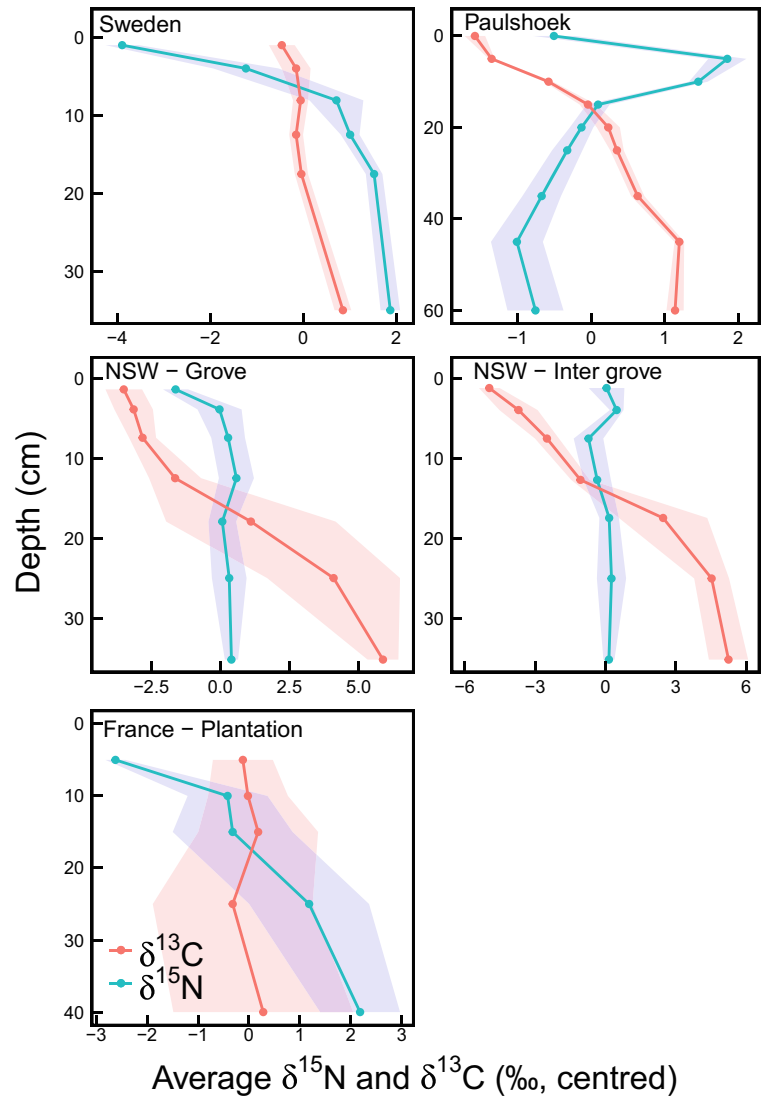
BRT analysis of the correlation between  $\delta^{13}\text{C}$  and  $\delta^{15}\text{N}$  values ranked CEC, mean diurnal temperature range, bulk density, MAT, clay and MAP as the top predictors (Fig. 4a), explaining 38% of the variance in the correlation between  $\delta^{13}\text{C}$  and  $\delta^{15}\text{N}$ . Partial dependency plots, which show the effect of a variable on the response after accounting for the average effects of all other variables in the model, of the BRT analysis of the soil profile correlations between  $\delta^{13}\text{C}$  and  $\delta^{15}\text{N}$  values (Fig. 5), showed that this was strongest at sites with  $\text{CEC} < 20 \text{ cmol kg}^{-1}$  and a mean diurnal temperature range  $< 13^\circ\text{C}$ . Sites with bulk density above  $1400 \text{ kg m}^3$  had strong correlation between soil  $\delta^{13}\text{C}$  and  $\delta^{15}\text{N}$  values. The influence of clay concentration on the correlation between  $\delta^{13}\text{C}$  and  $\delta^{15}\text{N}$  values was generally high. A number of sites with clay concentrations

between 30 and 35%, however, had a relative low influence of clay on the correlation. These sites were arid, receiving  $< 500 \text{ mm}$  mean annual precipitation and had a relatively poor correlation compared to mesic sites (i.e. between 500 and 1000 mm) with a moderate influence in hydric sites ( $> 1000 \text{ mm}$ ). The correlation between  $\delta^{13}\text{C}$  and  $\delta^{15}\text{N}$  values was stronger at sites with  $\text{MAT} > 19^\circ\text{C}$  (Supp. Fig. 4f).

#### Global geographic variation

Globally, soil  $\delta^{15}\text{N}$  values of surface soils were significantly positively correlated with  $\delta^{13}\text{C}$ , MAT and the prevalence of  $\text{C}_4$  photosynthetic vegetation and negatively correlated with CEC and diurnal T range (Table 2). Geospatial variation in global  $\delta^{13}\text{C}$  and  $\delta^{15}\text{N}$  values that were spatially averaged over  $0.1^\circ$  corresponded relatively well with each other at high latitudes ( $> 50^\circ$ ) where both  $\delta^{13}\text{C}$  and  $\delta^{15}\text{N}$  values were more negative compared to sites located nearer the equator (Fig. 5). Sites in which  $\delta^{13}\text{C}$  values were relatively high (Fig. 5) were from more arid regions such as Southern Africa, Australia and North America and in which  $\text{C}_4$  grass communities exist (Fig. 6).

**Fig. 3** Variation with soil depth of  $\delta^{13}\text{C}$  and  $\delta^{15}\text{N}$  values for sites in which  $\delta^{13}\text{C}$  and  $\delta^{15}\text{N}$  are poorly correlated with each other. The data was averaged for each depth and the confidence interval represented by the coloured bands calculated from the standard error. The  $\delta^{13}\text{C}$  and  $\delta^{15}\text{N}$  data were independently centred on 0 so as to allow comparison of the variation of these within a site. The range of the data corresponds to the original data



BRT analysis of global soil  $\delta^{15}\text{N}$  values (BRTglobal) ranked MAT,  $\delta^{13}\text{C}$ , CEC,  $C_4$ , diurnal range and MAP as the top predictors of soil  $\delta^{15}\text{N}$  (Fig. 4b), which explained 62% of the variation in  $\delta^{15}\text{N}$  values. The partial dependency plots for the BRTglobal (Supp. Fig. 5) showed that as MAT increased,  $\delta^{15}\text{N}$  values also increased. Sites with  $\delta^{13}\text{C}$  values below ca.  $-30\text{‰}$  had low  $\delta^{15}\text{N}$  values, which increased rapidly with increased  $\delta^{13}\text{C}$  values up until ca.  $-20\text{‰}$ , above which changes in  $\delta^{15}\text{N}$  values were relatively small. Therefore, much of the change in  $\delta^{15}\text{N}$  values associated with  $\delta^{13}\text{C}$  values occurred in a range of  $\delta^{13}\text{C}$  values considered to be characteristic of  $C_3$  dominated sites (Supp. Fig. 2). Sites with CEC values  $>10 \text{ cmol kg}^{-1}$  had relatively low soil  $\delta^{15}\text{N}$  values.  $\delta^{15}\text{N}$  values were also low for sites with

$<75\%$   $C_4$  vegetation. Soil  $\delta^{15}\text{N}$  values were reduced with increases in mean diurnal temperature range and generally with increased MAP (Supp. Fig. 5f).

Global  $\delta^{15}\text{N}$  values predicted from the full BRTglobal model, including both  $C_3$  and  $C_4$  sites, were strongly correlated with observed global  $\delta^{15}\text{N}$  values (Supp. Fig. 1). There was, however, a degree of under-prediction of  $\delta^{15}\text{N}$  values at low observed  $\delta^{15}\text{N}$  values and over-prediction at high observed  $\delta^{15}\text{N}$  values. Global soil  $\delta^{13}\text{C}$  values were bimodal with two ranges of  $\delta^{13}\text{C}$  values having peaks at  $-26.36\text{‰}$  and  $-17.58\text{‰}$ , indicating that there were a number of sites dominated by either predominantly  $C_3$  or  $C_4$  plants (Supp. Fig. 2). BRT's predicting global soil  $\delta^{15}\text{N}$  based on a subset of sites that were predominantly  $C_3$  dominated ranked



**Fig. 4** Relative influence of variables in determining the correlation between global soil  $\delta^{13}\text{C}$  and  $\delta^{15}\text{N}$  as determined by BRT analysis (a) as well as the relative influence of variables in determining the global soil  $\delta^{15}\text{N}$  as determined by BRT analysis (b). Values are the mean  $\pm$  SE of 10 runs of each model. Error bars represent standard error

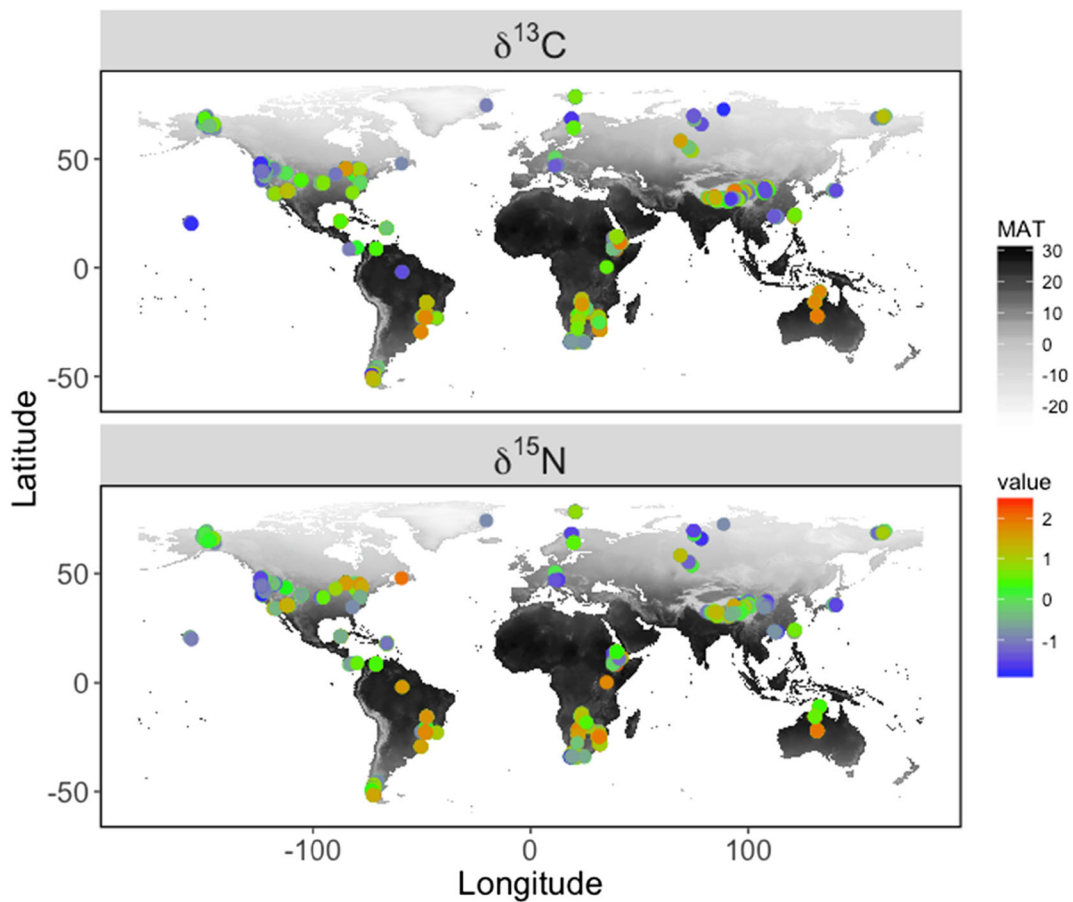
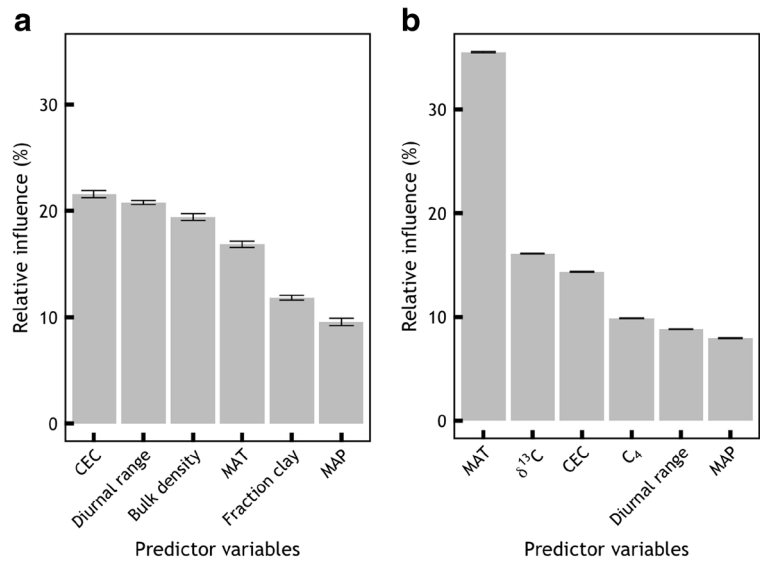


**Fig. 5** The global variation in soil  $\delta^{13}\text{C}$  and  $\delta^{15}\text{N}$ . The color of the points represents the site averages of  $\delta^{13}\text{C}$  and  $\delta^{15}\text{N}$  values standardized and centered to range between  $-1$  and  $1$ . Background fill colour represents mean annual temperature

**Table 2** Bivariate ranged major axis (RMA) analysis results of top six predictors of global soil  $\delta^{15}\text{N}$  with correlation coefficients ( $r$ ) shown with  $p$ -values (bold where significant). All variables used in the prediction of global soil  $\delta^{15}\text{N}$  are shown in Supp. Table 1

Predictor variables	n	r	p-value	Intercept	Slope
MAT	7461	0.48	< <b>0.001</b>	1.13	0.21
$\delta^{13}\text{C}$	5501	0.48	< <b>0.001</b>	14.16	0.43
CEC	7328	-0.2	< <b>0.001</b>	7.07	-0.15
% $\text{C}_4$	7415	0.43	< <b>0.001</b>	2.99	0.05
Diurnal T range	7456	-0.1	< <b>0.001</b>	5.82	-0.15
MAP	7474	-0.01	0.579	4.22	< 0.00

MAT,  $\delta^{13}\text{C}$ , CEC, bulk density, diurnal T range and MAP as top predictors (Supp. Table 2). The BRT developed for  $\text{C}_4$  dominated sites ranked MAT, CEC, bulk density, MAP, diurnal range and  $\delta^{13}\text{C}$  as top predictors. Although soil  $\delta^{13}\text{C}$  was found to be a strong predictor of  $\delta^{15}\text{N}$  for  $\text{C}_3$  sites, it was a weak predictor in  $\text{C}_4$  dominated sites.

## Discussion

This study suggests that either common or coordinated processes contribute to fractionation of soil C and N isotopes. The link between soil  $\delta^{13}\text{C}$  and  $\delta^{15}\text{N}$  values may inform understanding of these processes due to this coordination of soil processes determining both C and N isotope fractionation. Our results suggest that although the initial isotope composition of the organic matter is indisputably important, subsequent fractionation via soil processes, such as decomposition and related processes, may result in correlations between  $\delta^{13}\text{C}$  and  $\delta^{15}\text{N}$  values in geographic space and commonly following similar trajectories with soil depth. More positive  $\delta^{13}\text{C}$  and  $\delta^{15}\text{N}$  values with soil depth (Fig. 1) must result from increasing fractionation or more prolonged fractionation in deeper soils relative to shallower soils.

The importance of the vegetation characteristics in determining C isotopic composition is apparent from the bimodal distribution of soil  $\delta^{13}\text{C}$  values associated with  $\text{C}_3$  (-22‰ to -32‰; Troughton 1979) and  $\text{C}_4$  (-9.2‰ to -19.3‰; Hattersley 1982) vegetation (Fig. S2) whereas the variation in  $\delta^{13}\text{C}$  within the  $\text{C}_3$  and  $\text{C}_4$  groupings is caused by climatic and geographical factors

(Damesin et al. 1997). Likewise, global variation in soil  $\delta^{15}\text{N}$  values (Fig. 5) is associated with variation in foliar  $\delta^{15}\text{N}$  that varies with MAP, MAT, N availability, foliar N concentration, species composition and with the degree of  $\text{N}_2$  fixation (Craine et al. 2009). Organic matter enters soils in a diversity of ways and this influences the initial isotopic signature of soil C and N (Eissfeller et al. 2013). The majority of SOM, however, enters the soil as plant-derived detritus, where it is utilized by soil microbes (Berg and McClaugherty 2008) and decomposer fauna (Hättenschwiler and Gasser 2005). Consequently, the isotopic values of the dominant vegetation and the variation in  $\delta^{13}\text{C}$  and  $\delta^{15}\text{N}$  values, both between and within species (Damesin et al. 1997; Craine et al. 2015a), strongly influence SOM isotopic composition.

Unlike for C, however, there are also strong ecosystem feedbacks between soil and vegetation N in determining ecosystem  $\delta^{15}\text{N}$  values, because soil  $\delta^{15}\text{N}$  also partially determines plant  $\delta^{15}\text{N}$ . Despite this dependence of SOM isotopic composition on that of OM and vegetation, the variations in  $\delta^{13}\text{C}$  (range: -27.8 to -12.4‰) and  $\delta^{15}\text{N}$  (range: -0.1 to 10.1‰) with depth in soil profiles were often strongly correlated with each other (Table 1). Likewise, geospatial variation in global  $\delta^{13}\text{C}$  and  $\delta^{15}\text{N}$  values also corresponded relatively well across a wide range of climates and biomes (Fig. 5). For example,  $\text{C}_3$  and  $\text{C}_4$  dominated sites showed similar patterns of  $\delta^{13}\text{C}$  and  $\delta^{15}\text{N}$  enrichment through soil profiles (Fig. 2), although the range of values was smaller with  $\text{C}_4$  vegetation.

The correspondence between the increases of  $\delta^{13}\text{C}$  and  $\delta^{15}\text{N}$  values with depth is probably through processing of SOM, which is further supported by the most influential predictors in the BRT model for the correlation between  $\delta^{13}\text{C}$  and  $\delta^{15}\text{N}$  values through soil profiles (Fig. 4a), which themselves are related to microbial activity. Furthermore, soil  $\delta^{13}\text{C}$  values were also strong determinants of  $\delta^{15}\text{N}$  globally (regardless of soil and ecosystem type) while the remaining top predictors of  $\delta^{13}\text{C}$  could be related to SOM decomposition (Fig. 4b). Processing of SOM is determined by characteristics of the SOM, such as the C and N composition (Fernandez et al. 2003), as well as by environmental factors including soil temperature, moisture and aeration (Gholz et al. 2000; Zhang et al. 2008). The reason for the positive correlation between MAT and both  $\delta^{15}\text{N}$  and  $\delta^{13}\text{C}$  values could therefore be due to microbial activity increasing with increasing temperature. Mean diurnal temperature range (e.g. Li et al. 2011), CEC and soil

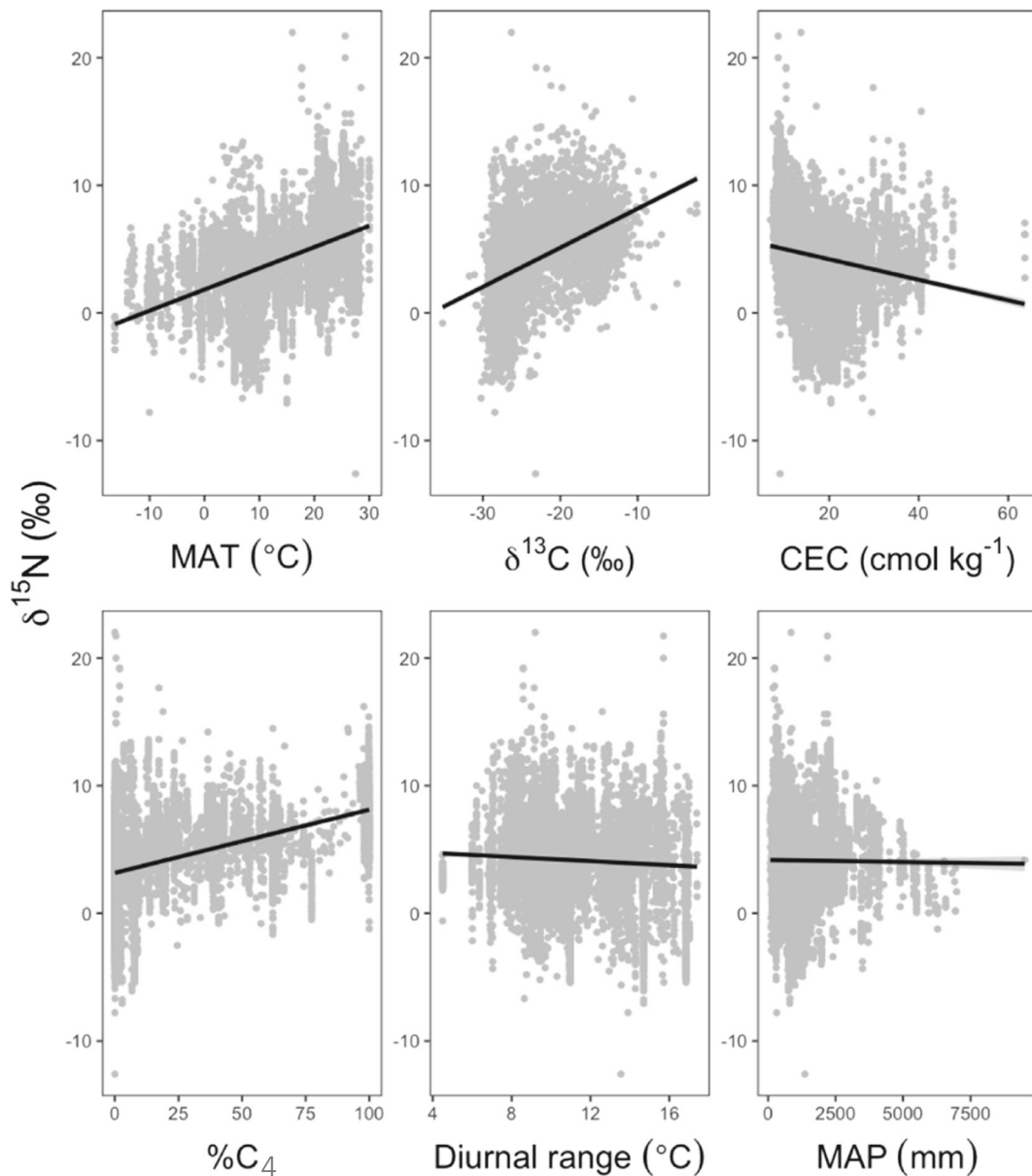


**Fig. 6** Bivariate analysis of the top six predictors of global soil  $\delta^{15}\text{N}$  against global soil  $\delta^{15}\text{N}$ . Lines indicate linear model function

fertility (Sikora 2013) may also be linked to SOM decomposition through soil microbial processes. Although favorable moisture conditions stimulate decomposer communities (Cotrufo et al. 2013), MAP was not significantly correlated with either  $\delta^{13}\text{C}$  or  $\delta^{15}\text{N}$  values at the global scale (Fig. 4b, Table 2). This is likely because many ecosystem properties depend on MAP obscuring clear relationships. For example, Craine et al. (2015a) related variation in global soil  $\delta^{15}\text{N}$  to variation in clay concentrations. Further, there is the

possibility that the limited range in MAP at the regional scale can obscure relationships between soil  $\delta^{15}\text{N}$  and MAP as the increase in soil  $\delta^{15}\text{N}$  with increasing MAP at the regional scale often breaks down at broader scales (Amundson et al. 2003; Austin and Vitousek 1998).

Despite strong global geographic correspondence between  $\delta^{13}\text{C}$  and  $\delta^{15}\text{N}$  and correspondence over soil depth (11 of 16 sites), some sites had non-significant (New South Wales, France, Sweden) or negative (Paulshoek) correlations between  $\delta^{13}\text{C}$

and  $\delta^{15}\text{N}$  (Fig. 3, Table 1). These sites indicate the complexity to the relationship between soil  $\delta^{13}\text{C}$  and  $\delta^{15}\text{N}$ , and dependence on other factors. For example, the New South Wales sites had a large proportion of  $\text{N}_2$ -fixing microbes in the surface soil (Macdonald et al. 2015) resulting in  $\delta^{15}\text{N}$  being close to 0‰. The non-significant Swedish and French sites were both associated with plantations (Boström et al. 2007; Zeller et al. 2007), whereas a corresponding natural site in France showed a significant relationship (Fig. 1). Paulshoek exhibited a maximum soil  $\delta^{15}\text{N}$  value at intermediated depths, which is indicative of N-loss during nitrification and denitrification (Hobbie and Ouimette 2009). This is not surprising as Paulshoek is arid with high soil temperatures and sporadic rainfall (Table 1) and these conditions increase nitrification/denitrification rates (Craine et al. 2015b). Thus despite the general global relationship between  $\delta^{13}\text{C}$  and  $\delta^{15}\text{N}$ , this correspondence does vary depending on local biotic, disturbance and environmental influences.

As a consequence of a link between soil  $\delta^{13}\text{C}$  and  $\delta^{15}\text{N}$ , interpretation of soil  $\delta^{13}\text{C}$  values as indicators of historical vegetation assemblages is complicated by the role of soil processes in determining soil  $\delta^{13}\text{C}$  values, as also shown by Wynn et al. 2005. The ranges of  $\delta^{13}\text{C}$  values with depth are commonly large (up to 11.0‰, Supp. Fig. 3) which overlaps the range of values commonly associated with vegetation change. For example,  $\delta^{13}\text{C}$  values between  $-16$  and  $-20$ ‰ have been used to indicate mixed  $\text{C}_3$  and  $\text{C}_4$  vegetation and  $> -16$ ‰ to indicate  $\text{C}_4$  dominance (Gillson 2015). From our study, however, whilst the minimum  $\delta^{13}\text{C}$  values of soils with  $\text{C}_3$  and  $\text{C}_4$  vegetation reflect the isotopic signature of the vegetation inputs, the maximum  $\delta^{13}\text{C}$  values are indistinguishable. Since the maximum  $\delta^{13}\text{C}$  values of soils supporting  $\text{C}_3$  vegetation overlap with the minimum  $\delta^{13}\text{C}$  values of  $\text{C}_4$  vegetation, interpretation of intermediate  $\delta^{13}\text{C}$  values (i.e.  $< \text{ca. } -15$ ‰) as indicating historical vegetation characteristics should be approached with caution. Furthermore, in order to demonstrate that ancient  $\delta^{13}\text{C}$  SOC values are indeed representative of ancient vegetation assemblages in samples of deep SOC, one must establish that the fraction of SOC remaining in the sample is very close to the original maximum concentration during soil formation and that fractionation has not been great (Wynn et al. 2006). This is because Rayleigh distillation and mixing processes vary with environmental and soil properties, with particularly strong effects associated with fine mineral

particles (i.e. clay) in fine grained soils (Krull and Skjemstad 2003; Wynn et al. 2005) and should not be assumed to be constant everywhere.

**Acknowledgements** This work was funded by the National Research Foundation (South Africa). We would like to thank Emma Grey, William Bond and Edmund February for providing data for the study.

## References

- Ågren GI, Bosatta E, Balesdent J (1996) Isotope discrimination during decomposition of organic matter: a theoretical analysis. *Soil Sci Soc Am J* 60:1121–1127. <https://doi.org/10.2136/sssaj1996.03615995006000040023>
- Amundson R, Austin AT, Schuur EA, Yoo K, Matzek V, Kendall C, Uebersax A, Brenner D, Baisden WT (2003) Global patterns of the isotopic composition of soil and plant nitrogen. *Glob Biogeochem Cycles*. <https://doi.org/10.1029/2002GB001903>
- Austin AT, Vitousek PM (1998) Nutrient dynamics on a precipitation gradient in Hawai'i. *Oecologia* 113(4):519–529
- Baisden WT, Amundson R, Brenner DL et al (2002) A multiisotope C and N modeling analysis of soil organic matter turnover and transport as a function of soil depth in a California annual grassland soil chronosequence. *Glob Biogeochem Cycles* 16:82–1–82–26. <https://doi.org/10.1029/2001GB001823>
- Balesdent J, Girardin C, Mariotti A (1993) Site-related (13) C of tree leaves and soil organic matter in a temperate Forest. *Ecology*. <https://doi.org/10.2307/1941808?ref=search-gateway:4f6368673c42b4f42edf719325fc510e>
- Benaglia T, Chauveau D, Hunter DR, Young DS (2009) Mixtools: an R package for analyzing finite mixture models. *J Stat Softw* 32:1–29
- Berg B, McClaugherty C (2008) Plant litter. Decomposition, humus formation, carbon sequestration, 2nd Ed. Springer, 2008.
- Berry JA, Collatz GJ, DeFries RS (2009) ISLSCP II C4 vegetation percentage
- Berry JA, Collatz GJ, DeFries RS (2009) ISLSCP II C4 vegetation percentage
- Billings SA, Richter DD (2006) Changes in stable isotopic values of soil nitrogen and carbon during 40 years of forest development. *Oecologia* 148:325–333. <https://doi.org/10.1007/s00442-006-0366-7>
- Boström B, Comstedt D, Ekblad A (2007) Isotope fractionation and  $^{13}\text{C}$  enrichment in soil profiles during the decomposition of soil organic matter. *Oecologia* 153: 89–98. <https://doi.org/10.1007/s00442-007-0700-8>
- Cerling TE (1984) The stable isotopic composition of modern soil carbonate and its relationship to climate. *Earth Planet Sci Lett* 71(2):229–240
- Chen Q, Shen C, Sun Y et al (2005) Spatial and temporal distribution of carbon isotopes in soil organic matter at the Dinghushan biosphere reserve, South China. *Plant Soil* 273: 115–128. <https://doi.org/10.2307/24125204?ref=no-x-route:bf8f8a632d5dc84e9c9ef56d558d465a>

- Collatz GJ, Berry JA, Clark JS (1998) Effects of climate and atmospheric CO<sub>2</sub> partial pressure on the global distribution of C<sub>4</sub> grasses: present, past, and future. *Oecologia* 114(4):441–454
- Cotrufo MF, Wallenstein MD, Boot CM et al (2013) The microbial efficiency-matrix stabilization (MEMS) framework integrates plant litter decomposition with soil organic matter stabilization: do labile plant inputs form stable soil organic matter? *Glob Change Biol* 19:988–995. <https://doi.org/10.1111/gcb.12113>
- Craine JM, Elmore AJ, Aida MPM et al (2009) Global patterns of foliar nitrogen isotopes and their relationships with climate, mycorrhizal fungi, foliar nutrient concentrations, and nitrogen availability. *New Phytol* 183:980–992. <https://doi.org/10.1111/j.1469-8137.2009.02917.x>
- Craine JM, Brookshire ENJ, Cramer MD, Hasselquist NJ, Koba K, Marin-Spiotta E, Wang L (2015a) Ecological interpretations of nitrogen isotope ratios of terrestrial plants and soils. *Plant Soil* 396(1–2):1–26
- Craine JM, Elmore AJ, WANG L et al (2015b) Convergence of soil nitrogen isotopes across global climate gradients. *Sci Rep* 5:8280–8288. <https://doi.org/10.1038/srep08280>
- Damesin C, Rambal S, Joffre R (1997) Between-tree variations in leaf delta C-13 of *Quercus pubescens* and *Quercus ilex* among Mediterranean habitats with different water availability. *Oecologia* 111:26–35
- DeFries RS, Hansen MC, Townshend JR, Janetos AC, Loveland TR (2000) A new global 1-km dataset of percentage tree cover derived from remote sensing. *Glob Chang Biol* 6(2): 247–254
- Dijkstra P, Ishizu A, Doucet R et al (2006) 13C and 15N natural abundance of the soil microbial biomass. *Soil Biol Biochem* 38:3257–3266. <https://doi.org/10.1016/j.soilbio.2006.04.005>
- Dormann CF, Elith J, Bacher S, Buchmann C, Carl G, Carré G, Marquéz JR, Gruber B, Lafourcade B, Leitão PJ, Münkemüller T (2013) Collinearity: a review of methods to deal with it and a simulation study evaluating their performance. *Ecography* 36(1):27–46
- Ehleringer JR, Buchmann N, Flanagan LB (2000) Carbon isotope ratios in belowground carbon cycle processes. *Ecol Appl* 10: 412–422
- Eissfeller V, Beyer F, Valtanen K et al (2013) Incorporation of plant carbon and microbial nitrogen into the rhizosphere food web of beech and ash. *Soil Biol Biochem* 62:76–81. <https://doi.org/10.1016/j.soilbio.2013.03.002>
- Ekblad A, Högberg P (2000) Analysis of δ13C of CO<sub>2</sub> distinguishes between microbial respiration of added C<sub>4</sub>-sucrose and other soil respiration in a C<sub>3</sub>-ecosystem. *Plant Soil* 219: 197–209. <https://doi.org/10.1023/A:1004732430929>
- Elith J, Leathwick JR, Hastie T (2008) A working guide to boosted regression trees. *J Anim Ecology* 77:802–813. <https://doi.org/10.1111/j.1365-2656.2008.01390.x>
- Esmeyjer-Liu AJ, Kürschner WM, Lotter AF, Verhoeven JT, Goslar T (2012) Stable carbon and nitrogen isotopes in a peat profile are influenced by early stage diagenesis and changes in atmospheric CO<sub>2</sub> and N deposition. *Water Air Soil Pollut* 223(5):2007–2022
- February EC, Higgins SI (2010) The distribution of tree and grass roots in savannas in relation to soil nitrogen and water. *S Afr J Bot* 76(3):517–523
- Fernandez I, Mahieu N, Cadisch G (2003) Carbon isotopic fractionation during decomposition of plant materials of different quality. *Global Biogeochem Cycles* 17:n/a–n/a. <https://doi.org/10.1029/2001GB001834>
- Fischer V, Joseph C, Tieszen LL, Schimel DS (2008) Climate controls on C<sub>3</sub> vs. C<sub>4</sub> productivity in North American grasslands from carbon isotope composition of soil organic matter. *Glob Chang Biol* 14(5):1141–1155
- Fry, B. (2006). *Stable isotope ecology* (Vol 521). New York: Springer
- Gabet EJ, Reichman OJ, Seabloom EW (2003) The effects of bioturbation on soil processes and sediment transport. *Annu Rev Earth Planet Sci* 31(1):249–273
- Gholz HL, Wedin DA, Smitherman SM et al (2000) Long-term dynamics of pine and hardwood litter in contrasting environments: toward a global model of decomposition. *Glob Change Biol* 6:751–765. <https://doi.org/10.1046/j.1365-2486.2000.00349.x>
- Gillson L (2015) Evidence of a tipping point in a southern African savanna? *Ecol Complex* 21:78–86. <https://doi.org/10.1016/j.ecocom.2014.12.005>
- Gillson L, Waldron S, Willis KJ (2004) Interpretation of soil delta(13)C as an indicator of vegetation change in African savannas. *J Veg Sci* 15:339–350
- Grey EF (2011) Some consequences of woody plant encroachment in a mesic South African savanna. Unpublished master's thesis, University of Cape Town, South Africa
- Handley LL, Raven JA (1992) The use of natural abundance of nitrogen isotopes in plant physiology and ecology. *Plant, Cell and Environment* 15:965–985. <https://doi.org/10.1111/j.1365-3040.1992.tb01650.x>
- Hargreaves GL, Hargreaves GH, Riley JP (1985) Irrigation water requirements for Senegal River Basin. *J Irrig Drain Eng - Asce* 111:265–275
- Hastie T, Friedman J, Tibshirani R (2001) Model assessment and selection. In *The elements of statistical learning*. Springer, New York, pp 193–224
- Hättenschwiler S, Gasser P (2005) Soil animals alter plant litter diversity effects on decomposition. *Proc Natl Acad Sci U S A* 102(5):1519–1524
- Hattersley PW (1982) δ13 values of C<sub>4</sub> types in grasses. *Funct Plant Biol* react-text 479(2):139–154
- Heil B, Ludwig B, Flessa H, Beese F (2000) 13C and 15N distributions in three spodic dystric cambisols under beech and spruce. *Isot Environ Health Stud* 36(1):35–47
- Hengl T, de Jesus JM, MacMillan RA et al (2014) SoilGrids1km — global soil information based on automated mapping. *PLoS One* 9:e105992–e105917. <https://doi.org/10.1371/journal.pone.0105992>
- Hijmans RJ, Van Etten J (2014) Raster: geographic data analysis and modeling. R package version 2.2-31. URL <http://CRAN.R-project.org/package=raster>. Accessed 15 Mar 2014
- Hijmans RJ, van Etten J, Cheng J, Mattiuzzi M, Sumner M, Greenberg JA, Lamigueiro OP, Bevan A, Racine EB, Shortridge A, Hijmans MR (2015) Package ‘raster’. R package
- Hobbie EA, Ouimette AP (2009) Controls of nitrogen isotope patterns in soil profiles. *Biogeochemistry* 95:355–371. <https://doi.org/10.1007/s10533-009-9328-6>
- Hobbie EA, Macko SA, Shugart HH (1999) Insights into nitrogen and carbon dynamics of ectomycorrhizal and saprotrophic fungi from isotopic evidence. *Oecologia* 118:353–360

- Hobbie EA, Macko SA, Williams M (2000) Correlations between foliar  $\delta^{15}\text{N}$  and nitrogen concentrations may indicate plant-mycorrhizal interactions. *Oecologia* 122(2):273–283
- Hogberg P (1997) Tansley review no. 95:  $^{15}\text{N}$  natural abundance in soil-plant systems. (erratum: July 1998, v. 139 (3), p. 595.). *New Phytol* 1–26
- Huang Y, Bol R, Harkness DD, Ineson P, Eglinton G (1996) Post-glacial variations in distributions,  $^{13}\text{C}$  and  $^{14}\text{C}$  contents of aliphatic hydrocarbons and bulk organic matter in three types of British acid upland soils. *Org Geochem* 24(3):273–287
- Krull ES, Skjemstad JO (2003)  $\delta^{13}\text{C}$  and  $\delta^{15}\text{N}$  profiles in 14 C-dated Oxisol and Vertisols as a function of soil chemistry and mineralogy. *Geoderma* 112(1):1–29
- Kuzyakov Y, Domanski G (2000) Carbon input by plants into the soil. *Rev J Plant Nutr Soil Sci* 163(4):421–431
- Kuzyakov Y, Mitusov A, Schneckenberger K (2006) Effect of C3–C4 vegetation change on  $\delta^{13}\text{C}$  and  $\delta^{15}\text{N}$  values of soil organic matter fractions separated by thermal stability. *Plant Soil* 283:229–238. <https://doi.org/10.1007/s11104-006-0015-2>
- Lang DT, Lang M (2016) Package “RCurl”, R package
- Lerch TZ, Nunan N, Dignac MF et al (2011) Variations in microbial isotopic fractionation during soil organic matter decomposition. *Biogeochemistry* 106:5–21. <https://doi.org/10.2307/41490503?ref=no-x-route:12af3dd2e718256c638206e697516b1e>
- Li Z, Wang X, Zhang R et al (2011) Contrasting diurnal variations in soil organic carbon decomposition and root respiration due to a hysteresis effect with soil temperature in a *Gossypium s.* (cotton) plantation. *Plant Soil* 343:347–355. <https://doi.org/10.1007/s11104-011-0722-1>
- Liu J, Wang C, Peng B, Xia Z, Jiang P, Bai E (2017) Effect of nitrogen addition on the variations in the natural abundance of nitrogen isotopes of plant and soil components. *Plant Soil* 412(1–2):453–464
- Lu H, Wu N, Gu Z et al (2004) Distribution of carbon isotope composition of modern soils on the Qinghai-Tibetan plateau. *Biogeochemistry* 70:273–297. <https://doi.org/10.2307/4151469?ref=no-x-route:06baab149dad744f1af8e19b479345cc>
- Macdonald BCT, Warneke S, Maïson E, McLachlan G, Farrell M (2015) Spatial decoupling of soil nitrogen cycling in an arid chenopod pattern ground. *Soil Res* 53(1):97–104
- Maechler M (2015) Diptest: Hartigan’s dip test statistic for Unimodality—corrected. URL <http://CRAN.R-project.org/package=diptest>. R package version 0.75-7
- Marin-Spiotta E, Smith AP, Atkinson EE, Chaopricha NT (2014) Landscape disturbance history and belowground carbon dynamics. In: AGU fall meeting abstracts 2014 Dec, vol. 1. p L04
- Mariotti A, Germon JC, Hubert P et al (1981) Experimental determination of nitrogen kinetic isotope fractionation: some principles; illustration for the denitrification and nitrification processes. *Plant Soil* 62:413–430. <https://doi.org/10.2307/42935413?ref=search-gateway:51f8021df01bde84558143257f594a9b>
- Ometto JPHB, Ehleringer JR, Domingues TF, Berry JA, Ishida FY, Mazzi E, Higuchi N, Flanagan LB, Nardoto GB, Martinelli LA (2006) The stable carbon and nitrogen isotopic composition of vegetation in tropical forests of the Amazon Basin, Brazil. *Nitrogen Cycling in the Americas: Natural and Anthropogenic Influences and Controls*. Springer, New York, pp 251–274
- Parton W, Silver WL, Burke IC et al (2007) Global-scale similarities in nitrogen release patterns during long-term decomposition. *Science* 315:361–364. <https://doi.org/10.1126/science.1134853>
- Pataki DE, Billings SA, Naumburg E, Goedhart CM (2008) Water sources and nitrogen relations of grasses and shrubs in phreatophytic communities of the Great Basin desert. *J Arid Environ* 72:1581–1593. <https://doi.org/10.1016/j.jaridenv.2008.03.011>
- Ponsard S, Ardit R (2000) What can stable isotopes ( $\delta^{15}\text{N}$  and  $\delta^{13}\text{C}$ ) tell about the food web of soil macro-invertebrates? *Ecology* 81(3):852–864
- Pries CEH, Schuur EA, Crummer KG (2012) Holocene carbon stocks and carbon accumulation rates altered in soils undergoing permafrost thaw. *Ecosystems* 15(1):162–173
- Qiao Y, Miao S, Silva LC, Horwath WR (2014) Understorey species regulate litter decomposition and accumulation of C and N in forest soils: a long-term dual-isotope experiment. *For Ecol Manag* 329:318–327
- Ramankutty N, Foley JA (1998) Characterizing patterns of global land use: an analysis of global croplands data. *Glob Biogeochem Cycles* 12(4):667–685
- Ridgeway G, Southworth MH, RUnit S (2013) Package “gbm”, R package.
- Rovira P, Vallejo VR (2002) Labile and recalcitrant pools of carbon and nitrogen in organic matter decomposing at different depths in soil: an acid hydrolysis approach. *Geoderma* 107(1):109–141
- Sikora F J, Moore KP (2014) Soil test methods from the southeastern United States. S. Coop. Ser. Bul, (419). Clemson University, Clemson
- Silfer JA, Engel MH, Macko SA (1992) Kinetic fractionation of stable carbon and nitrogen isotopes during peptide bond hydrolysis: experimental evidence and geochemical implications. *Chem Geol Isot Geosci section* 101:211–221. [https://doi.org/10.1016/0009-2541\(92\)90003-N](https://doi.org/10.1016/0009-2541(92)90003-N)
- Sollins P, Kramer MG, Swanston C et al (2009) Sequential density fractionation across soils of contrasting mineralogy: evidence for both microbial- and mineral-controlled soil organic matter stabilization. *Biogeochemistry* 96:209–231. <https://doi.org/10.1007/s10533-009-9359-z>
- Swap RJ, Aranibar JN, Dowty PR (2004) Natural abundance of  $^{13}\text{C}$  and  $^{15}\text{N}$  in C3 and C4 vegetation of southern Africa: patterns and implications. *Global change ...* <https://doi.org/10.1046/j.1529-8817.2003.00702.x>
- Troughton JH (1979)  $\delta^{13}\text{C}$  as an indicator of carboxylation reactions. In *Photosynthesis II*. Springer Berlin, Heidelberg, pp 140–149
- Trumbore S (2009) Radiocarbon and soil carbon dynamics. *Annu Rev Earth Planet Sci* 37:47–66
- Wallander H, Nilsson LO, Hagerberg D, Rosengren U (2003) Direct estimates of C:N ratios of ectomycorrhizal mycelia collected from Norway spruce forest soils. *Soil Biol Biochem* 35:997–999. [https://doi.org/10.1016/S0038-0717\(03\)00121-4](https://doi.org/10.1016/S0038-0717(03)00121-4)
- Wickham H (2009) ggplot2: elegant graphics for data analysis. Springer Science & Business Media, Berlin

- Wilson AT, Grinsted MJ (1977)  $^{12}\text{C}/^{13}\text{C}$  in cellulose and lignin as palaeothermometers. *Nature* 265(5590):133–135
- Wynn JG, Bird MI, Wong VNL (2005) Rayleigh distillation and the depth profile of  $^{13}\text{C}/^{12}\text{C}$  ratios of soil organic carbon from soils of disparate texture in iron range National Park, Far North Queensland, Australia. *Geochim Cosmochim Acta* 69:1961–1973. <https://doi.org/10.1016/j.gca.2004.09.003>
- Wynn JG, Harden JW, Fries TL (2006) Stable carbon isotope depth profiles and soil organic carbon dynamics in the lower Mississippi Basin. *Geoderma* 131:89–109. <https://doi.org/10.1016/j.geoderma.2005.03.005>
- Zeller B, Brechet C, Maurice JP, Le Tacon F (2007)  $\delta^{13}\text{C}$  and  $\delta^{15}\text{N}$  isotopic fractionation in trees, soils and fungi in a natural forest stand and a Norway spruce plantation. *Ann For Sci* 64(4):419–429
- Zhang D, Hui D, Luo Y, Zhou G (2008) Rates of litter decomposition in terrestrial ecosystems: global patterns and controlling factors. *J Plant Ecol* 1:85–93. <https://doi.org/10.1093/jpe/rtn002>